Subunit *b*-Dimer of the *Escherichia coli* ATP Synthase Can Form Left-Handed Coiled-Coils

John G. Wise and Pia D. Vogel
Department of Biological Sciences, Southern Methodist University, Dallas, Texas 75275-0376

ABSTRACT One remaining challenge to our understanding of the ATP synthase concerns the dimeric coiled-coil stator subunit *b* of bacterial synthases. The subunit *b*-dimer has been implicated in important protein interactions that appear necessary for energy conservation and that may be instrumental in energy conservation during rotary catalysis by the synthase. Understanding the stator structure and its interactions with the rest of the enzyme is crucial to the understanding of the overall catalytic mechanism. Controversy exists on whether subunit *b* adopts a classic left-handed or a presumed right-handed dimeric coiled-coil and whether or not staggered pairing between nonhomologous residues in the homodimer is required for intersubunit packing. In this study we generated molecular models of the *Escherichia coli* subunit *b*-dimer that were based on the well-established heptad-repeat packing exhibited by left-handed, dimeric coiled-coils by employing simulated annealing protocols with structural restraints collected from known structures. In addition, we attempted to create hypothetical right-handed coiled-coil models and left- and right-handed models with staggered packing in the coiled-coil domains. Our analyses suggest that the available structural and biochemical evidence for subunit *b* can be accommodated by classic left-handed, dimeric coiled-coil quaternary structures.

INTRODUCTION

The F_1F_0 ATP synthases catalyze the condensation of ADP and Pi to form ATP and water. These ubiquitous enzymes are responsible for the majority of ATP production under aerobic conditions. The energy input for this highly endergonic reaction is an electrochemical gradient of protons across a membrane that is generally provided by either oxidative or photorespiratory systems. ATP synthases consist of an integral membrane sector F_0 that contains the sites for proton translocation and a more peripheral F_1 sector that contains nucleotide binding sites that include the catalytic sites. The actual synthesis of ATP by F_1F_0 involves a novel rotary mechanism in which proton flow through the F_0 complex drives rotation of subunits in F_0 and F_1. These rotary movements serve to drive the binding of substrates and the release of products from the catalytic sites (see (1–5) for reviews).

The peripherally bound F_1 complex from *Escherichia coli* is composed of five subunits in an $\alpha_3\beta_3\gamma\delta\varepsilon$ arrangement. The F_0 sector of *E. coli* ATP synthase consists of three different subunits, *a*, *b*, and *c*, in a 1:2:10 stoichiometric ratio. The α and β subunits of F_1 form an alternating hexameric structure surrounding the γ subunit, with the ε subunit interacting with γ near the membrane to form an internal central stalk within the F_1 hexamer. Subunit δ is thought to interact with the C-terminal end of a dimer of *b*-subunits to form a stator structure or external stalk. The external and internal stalks connect the F_1 and F_0 sectors to each other. Subunit *b* is membrane embedded at the N-terminus and forms a peripheral stalk after leaving the membrane where it is attached to F_1 at its C-terminus. Dimerization of subunit *b* appears to be required for proper assembly and function of the ATP synthase complex. The dimeric structure of *b* has been studied using a variety of biophysical and biochemical techniques, including electron spin resonance spectroscopy, circular dichroism, chemical cross-linking, and sedimentation studies. (See (4,6–9) for reviews.)

Some high resolution structural information is available for *E. coli* subunit *b*, but it is limited to an NMR study of a 33-residue monomeric segment of the membrane-spanning N-terminal region (9) and an x-ray study of a 61-residue monomeric segment (residues 62–122) reported in Del Rizzo et al. (10). The latter 61-residue monomer structure has been dubbed the ''dimerization domain'' by Dunn and co-workers since it contributes to the dimerization of subunit *b*. Supporting earlier results using circular dichroism, both the NMR and the x-ray structures showed those portions of *b* to be highly α-helical. Unfortunately, direct dimeric interactions could not be deduced from either the NMR study on the transmembrane monomer or the crystallographic study on the dimerization domain monomer.

Although there is general consensus that the extensive evidence accumulated to date suggests that the *b*-subunit forms an elongated, parallel, dimeric α-helical structure throughout much of the peripheral stalk region, there is controversy about whether this peripheral stalk is predominantly a conventional left-handed coiled-coil structure as originally described by Crick (11) or an unconventional right-handed, dimeric, coiled-coil structure as recently claimed by Del Rizzo et al. (10,12). The proposed right-handed coiled-coil structure of Del Rizzo et al. is based on the slight right-handed twist observed for apolar residues in the dimerization

Submitted August 30, 2007, and accepted for publication January 29, 2008.

Address reprint requests to Pia D. Vogel, Dept. of Biological Sciences, Southern Methodist University, Dallas, TX, Tel.: 214-768-1790; Fax: 214-768-3955; E-mail: pvogel@smu.edu.

Editor: David D. Thomas.

0006-3495/08/06/5040/13 $2.00

doi: 10.1529/biophysj.107.121012

domain of the crystallized monomer (10), the reported undecad repeat of apolar residues in this region of *b* (12), and the propensity of certain cysteine substitution mutations in *b* to form disulfide bonds that are offset in sequence (12). A potential offset between monomers was also discussed as one explanation for intersubunit distances obtained from double electron electron resonance spectroscopy experiments using specifically spin-labeled subunits *b* in reconstituted *E. coli* ATP synthase (13). Dimeric right-handed coiled-coils, with or without an offset, have not yet been directly observed.

Crick's predictions of left-handed coiled-coil dimers composed of two very slightly deformed parallel α-helices crossing at about a 20° angle to each other, an angle that results in helices that ''slowly wind round each other'' and that are stabilized by the occurrence of a repeating heptad of amino acid side-chain ''knobs'' falling into side-chain created ''holes'' (11), have been verified hundreds of times in high resolution protein structures to date. A number of bioinformatics methods based on sequence analysis for the prediction of these coiled-coil heptad repeat structures have been developed and used with much success (14–18). In addition, a number of modeling techniques have also been successfully employed to build theoretical coiled-coil structures that implement by molecular mechanics techniques the optimization of the geometries first identified by Crick (as in Harbury et al. (19)) or that use simulated annealing (SA) protocols that are restrained by Crick's geometries (as in Nilges and Brünger (20) and Charest and Lavigne (21)).

Several general questions can be raised about the structural arrangements of subunit *b*-dimers and, more specifically, about the validity of the unusual staggered, right-handed coiled-coil arrangement proposed by Del Rizzo et al. (10,12). First, are there any alternatives to the subunit *b* undecad repeats proposed in Del Rizzo et al. (12)? Second, can subunit *b* reasonably and stably adopt a conventional nonstaggered, left-handed coiled-coil structure as described by Crick (11)? Third, can the ''slight right-handed twist'' observed in the crystal structure of truncated subunit *b*-monomer (10) be accommodated by a dimeric left-handed coiled-coil structure or can the crystal structure only be accommodated by right-handed coiled-coil structures? Fourth, can theoretical dimeric, right-handed coiled-coil structures be identified that might serve as test structures for hypothetical right-handed and right-handed staggered coiled-coils? Finally, is a staggered start in the coiled-coil structure necessary for structural stability of the subunit *b*-dimer?

This study was undertaken to investigate these questions about the stator *b*-dimer of the *E. coli* ATP synthase. We used molecular modeling techniques based on the theoretical methods first enumerated by Crick (11) that have been applied in Nilges and Brünger (20) and more recently in Charest and Lavigne (21). By combining SA modeling approaches with the recent advances in sequence prediction of dimeric coiled-coil proteins, we have been able to create a number of models of the *E. coli* subunit *b*-dimer that suggest a left-handed coiled-coil structure with no offset in amino acid residue interactions between residues 31 and 116 can stably form and may be the preferred dimeric structure for the *E. coli* subunit *b* stator. In addition, we present evidence that theoretical left-handed and right-handed coiled-coil dimeric structures that contain a staggered coiled-coil region can both accommodate the results of cysteine cross-linking studies previously used to support the claim that the subunit *b*-dimer must exist as a right-handed coiled-coil.

METHODS

Prediction of heptad repeats in the subunit *b* amino acid sequence was performed with the *paircoil2* program (18), using a sequence window size of 28, or the *multicoil* program (16). Extensive use of the Visual Molecular Dynamics (VMD) suite of programs (22) for the visualization and analysis of protein structures was made. The extraction of distance and dihedral data from known protein structures was performed using the Tcl/Tk (23) and Python (24) scripting interfaces incorporated into VMD.

Ab initio SA experiments using restraint data extracted from known proteins were performed with the XPLOR-NIH program suite, versions 2.11–2.18 (25,26) essentially as described in Nilges et al. (27). The protein topology and parameter files used were the included XPLOR versions, protein-1.0.par and protein-1.0.top. The XPLOR-NIH program was serially run on a Linux computing cluster utilizing between 20 and 44 nodes. Individual structures were calculated by each employed node in parallel, and 20–48 structures were calculated in each set of experiments. The starting protein structure and initial coordinate files having an arbitrary extended conformation with ideal geometry were generated by XPLOR-NIH based only on the amino acid sequence of the subunit *b* protein and the XPLOR topology and parameter files. Each of the protein structures produced by the initial SA protocol was subsequently refined by slow cooling protocols that had softened van der Waals repulsions.

These refinement protocols were essentially identical to those originally written for XPLOR (28) by Michael Nilges, John Kuszewski, and Axel T. Brünger. After completion of the refinement protocols, each of the structures was analyzed by additional XPLOR-NIH protocols that quantified any distance and dihedral restraint violations and examined the geometry of the protein. ''Acceptable'' structures for this work were minimally defined as having no distance restraint violations >2 Å or dihedral restraint violations $>5°$. ''Acceptable'' protein structure geometries were defined as having no deviations from ideal bond lengths >0.1 Å and no deviations from ideal bond angles or impropers $>5°$. Independent stereochemical quality checks were performed on the acceptable proteins using the PROCHECK v 3.5.4 analysis suite originally described in Morris et al. (29) and Laskowski et al. (30).

Energy minimizations and short dynamics experiments were performed in the nanoscale molecular dynamics molecular dynamics program described in Phillips et al. (31). The calculation of electrostatic charges on proteins was performed using the python script developed in Dolinsky et al. (32). Solvent-accessible surface representations were calculated by the MSMS program of Sanner et al. (33). The computers used were Intel Pentium P4 32-bit single CPU units running OpenSuse10 or Scientific Linux 5.0 and a 44-CPU Linux computing cluster with either Scientific Linux 5.0 or FedoraCore 4 Linux operating systems.

RESULTS

Analysis of known left-handed, parallel, coiled-coil dimeric proteins to create restraint tables for building subunit *b* models

To model the ATP synthase dimeric subunit *b* coiled-coil domain, seven entries in the PDB that have well-character-

ized, parallel, left-handed coiled-coil domains—cortexillin I (34), the N-terminal dimerization domain of the APC tumor suppressor (35), the conserved segments 1A and 2B of the intermediate filament dimer (36), part of the MAD1-MAD2 core complex (37), part of the muscle α-tropomyocin (38), the early endosome autoantigen 1 C-terminus (39), and part of the myosin rod (40)—were analyzed within their coiled-coil domains to generate a set of ideal distance and dihedral restraints for modeling left-handed coiled-coil domains. Sequence-based predictions of the coiled-coil domains from these proteins were performed using the program *paircoil2* (18) and *multicoil* (16). Those sequence regions identified as having a high probability of being coiled-coil were checked visually after loading the respective protein structures in VMD. Structures having a *paircoil2* P-score of <0.045 (18) and a dimeric coiled-coil probability determined by *multicoil* >0.7 (16) were then used to generate averaged modeling distance and dihedral angle restraints for ideal left-handed coiled-coil dimerization domains.

Initially, interchain Cα-Cα, Cβ-Cβ, and Cγ-Cγ distances relative to the identified coiled-coil heptad positions (*a, b, c, d, e, f*, and *g*) were collected using Tcl scripts programmed for this purpose. In addition, intrachain peptidyl amide to peptidyl carbonyl distances and longer range Cα to Cα at intervals of 10 and 20 residues were also analyzed. These latter Cα to Cα + 10 and Cα to Cα + 20 intervals were found to be useful for ensuring that extended conformations of the coiled-coils were produced in the subsequent SA experiments. In addition to these distances, ϕ and ψ dihedral angles were determined for each of the identified coiled-coil domains in the ideal protein set. The data collected for each of the distances and angles discussed above for the seven coiled-coil heptad positions *a–g* for each of the protein structures were then averaged for all identified heptad positions in the set (see Table 1).

Simulated annealing experiments to test the ideal restraint database set

The data in Table 1 were used to create distance restraint tables for the generation of ideal parallel, left-handed dimeric proteins by ab initio SA protocols as described in Methods. Initially, a number of different experiments were performed using different combinations of restraint data as well as different fractional values of the individual restraint values used for plus and minus restraint variances. These experiments were performed on the cortexillin I coiled-coil domain protein sequence in an attempt to recreate the reported cortexillin I coiled-coil three-dimensional structure from only sequence, the ideal atom to atom distances, and dihedral angle restraint data shown in Table 1. Typically, in each of these preliminary experiments, 30–50 refined protein structures were created by SA for each different combination of restraints and variances. SA using the particular set of restraints and plus-minus variances to be tested was subsequently performed to generate sets of multiple structures. After completion of the refinement protocol, acceptance protocols were performed on all of the structures to rank the quality of each model with respect to distance and dihedral restraints employed, as well as any deviations from ideal bond length, bond angle, and improper geometries. The model structures with the lowest number of restraint and geometry violations and lowest total energy as calculated by XPLOR-NIH were chosen for further analysis.

The best combinations of restraints and variances were identified by comparing the best SA models produced under different restraint combinations to the reported crystal structure of cortexillin I (34). Because of the long, extended nature of the coiled-coil domains produced by our modeling protocols (no long-distance structural information was used other than the restraint distances of 15 and 30 Å between every 10th and 20th Cα atom) and the fact that the models were produced de novo with no starting protein structure, simple comparison of homologous atom positions after superposition on the crystal structure by, for example, root mean square deviation (RMSD) analysis of backbone atoms was not found to be very useful for quantitatively judging the best modeling conditions. The most probable reason for this is that slight deviations of the coiled-coil helical axis from the theoretical ideal occurred at some point in the structure that then produced relatively large displacements of atoms further down the coiled helices.

This problem of small local changes producing larger overall deviations in coiled-coil structures is not unique to

TABLE 1 Distances and dihedrals determined from the ideal coiled-coil data set

Measurement	Heptad a	Heptad b	Heptad c	Heptad d	Heptad e	Heptad f	Heptad g
Distance Cα-Cα	5.6 ± 0.6	12.6 ± 0.6	13.4 ± 0.5	6.5 ± 0.5	9.0 ± 0.7	14.0 ± 0.6	10.2 ± 0.6
Distance Cβ-Cβ	5.4 ± 0.6	15.1 ± 0.6	14.3 ± 0.6	4.2 ± 0.5	10.9 ± 0.7	16.1 ± 0.7	9.7 ± 0.6
Distance Cγ-Cγ	5.4 ± 1.4	16.5 ± 1.1	16.2 ± 1.0	5.3 ± 0.8	10.7 ± 1.2	18.1 ± 0.7	11.2 ± 1.3
Dihedral ϕ	−62.7 ± 7.6	−62.9 ± 9.5	−62.5 ± 6.0	−65.7 ± 8.9	−62.9 ± 5.6	−66.3 ± 7.9	−63.8 ± 7.6
Dihedral ψ	−43.3 ± 8.2	−43.1 ± 7.2	−42.5 ± 8.4	−40.4 ± 7.1	−38.8 ± 8.3	−43.2 ± 9.0	−40.6 ± 8.0

Distances are given in Å. Dihedral angles are presented in degrees. The plus/minus values indicated represent one standard deviation from the mean. The interchain Cα to Cα and Cβ to Cβ atom distances were calculated from at least 72 data points for each heptad position, and the Cγ to Cγ atom distances were calculated from at least 68 data points for each heptad position. The average ϕ dihedral angle for all heptad positions was $-63.7° \pm 7.8°$, and the average ψ dihedral angle was $-41.7° \pm 8.2°$.

our modeling. As pointed out earlier (41), NMR determination of the structures of coiled-coil proteins can be difficult since ''without long-range information, small inaccuracies in the structure determination can be propagated into large deviations over the length of the coiled-coil''. Since we do not yet have any definitive long-range information for the structure of the *E. coli* ATP synthase subunit *b*-dimer, we purposefully tried to limit the introduction of any arbitrary long-range information into our modeling protocols. Instead of using superposition and RMSD analysis, we used quantification of Cα to Cα distances and ϕ and ψ dihedral angles in the models (as in Table 1) and comparison of these values to the values obtained from the crystal structure of cortexillin I to choose the best combination of restraints and variances for subsequent work.

Initially nine different combinations of restraints (Cα- Cα, Cβ-Cβ, and/or Cγ-Cγ distances and ϕ and ψ dihedral restraints, including different values of plus-minus variances on those restraints) were tested, and the best structures produced were analyzed as described (data not shown). The combination that had the best compromise between least violations of distance and dihedral restraints and that produced the model with lowest energy used distance restraints between homologous heptad Cα atoms with an allowed $\pm$25% variation and ϕ and ψ angle restraints set to $-63.7\% \pm 15\%$ and $-41.7\% \pm 15\%$, respectively. Table 2 shows the results of the measurement of Cα to Cα distances and ϕ and ψ dihedral angles for the best modeled cortexillin I model. These values can be compared to the same distances and angles measured from the reported crystal structure of this protein shown in Table 3. For ease of comparison, the differences between the best model and the reported crystal structure are shown in Table 4. It can be seen from these results that the modeled protein was very similar to the crystal structure in terms of the differences in distance between Cα atoms of the seven heptad positions ($\leq \pm 1.4$ Å, Table 4). The largest deviations were in the most closely packed regions of the coiled-coil interface (the *a* and *d* heptad positions). This was not surprising since the interface regions of the dimer have the most difficulty satisfying stereochemical and steric environments. Differences in the ϕ and ψ dihedral angles measured between the model and reported crystal structure were $<10\%$ (Table 4).

Using the restraint combinations identified in these preliminary experiments, the SA protocol we employed reproduced a structural model of the cortexillin I dimer (34) that very closely resembled the reported crystal structure (Fig. 1). The left panel of the figure shows the superposed helical structures of the modeled dimer of cortexillin I (shown in *red*) and the cortexillin I crystal structure (shown in *blue*). The center panel shows a view taken at $\sim 90°$ from the first two views. This latter image demonstrates that the modeled structure does not have the very straight coiled-coil helical axis present in the crystal structure and serves to demonstrate the problem of judging the model quality by RMSD of backbone atoms as discussed above. For reference, the overall backbone atom RMSD on these two structures was 6.0 Å.

The hypotheses that the cortexillin I model produced by our SA protocol represents a structure that is packed very similarly to the reported crystal structure and that the backbone deviations represented by the overall RMSD of 6.0 Å indicates inaccuracies in the long-range helical axis superposition (as visually suggested by Fig. 1 *center*) are supported by additional calculations of RMSDs on localized sections of the two structures. When backbone RMSD values for the best SA modeled and reported crystal structures for cortexillin I that represented consecutive stretches of 10, 20, or 30 amino acid residues of both chains were calculated, mean RMSD values of 1.4 ± 0.4, 1.7 ± 0.5, and 1.9 ± 0.2 were respectively observed. These calculations strongly suggest that the modeling of the local packing between the helices of the cortexillin I left-handed coiled-coil dimer was quite accurate at any given point in the structure and that the inaccuracies were dominated by propagation of small local inaccuracies over long ranges, as suggested in Schnell et al. (41).

Fig. 1 (*right panel*) shows the solvent-accessible molecular surface of these two structures as drawn by the MSMS program of Sanner et al. (33) colored by charge as calculated in Dolinsky et al. (32), with red representing negative charge and blue representing positive charges. The similarities between the modeled and crystal structures are especially apparent in these views. In the surface representation, the similarities are exact enough that even the ''hole'' in the packing in the middle of the crystal structure is reproduced in the model produced by SA. The quality of this ab initio, sequence-only produced model was thus deemed sufficiently good to continue on our goal of modeling the ATP synthase subunit *b*-dimer.

TABLE 2 Modeled cortexillin I (1D7M) based on averaged restraints obtained from the ideal coiled-coil data set

Measurement	Heptad a	Heptad b	Heptad c	Heptad d	Heptad e	Heptad f	Heptad g
Distance Cα-Cα	7.0 ± 0.3	12.6 ± 1.5	13.4 ± 1.8	8.0 ± 0.3	9.9 ± 1.0	14.1 ± 1.7	10.8 ± 1.5
Dihedral ϕ	-60.0 ± 6.1	-62.2 ± 7.7	-64.9 ± 8.3	-58.5 ± 6.4	-60.3 ± 6.4	-65.2 ± 8.2	-64.2 ± 7.0
Dihedral ψ	-37.2 ± 3.6	-41.0 ± 4.7	-42.7 ± 4.8	-40.3 ± 5.1	-39.1 ± 5.2	-42.4 ± 5.1	-42.4 ± 5.1

Distances are given in Å. Dihedral angles are presented in degrees. The plus/minus values indicated represent one standard deviation from the mean. The overall average ϕ dihedral angle was $-62.5° \pm 6.5°$, and the overall average ψ dihedral angle was $-40.7° \pm 4.8°$.

TABLE 3 Data from the cortexillin I (1D7M) crystal structure (as a reference for the 1D7M model in Table 2)

Measurement	Heptad a	Heptad b	Heptad c	Heptad d	Heptad e	Heptad f	Heptad g
Distance Cα-Cα	5.6 ± 0.6	12.7 ± 0.6	13.6 ± 0.5	6.8 ± 0.5	9.1 ± 0.6	14.3 ± 0.6	10.6 ± 0.5
Dihedral ϕ	−60.1 ± 6.1	−57.4 ± 8.2	−57.8 ± 5.8	−63.3 ± 8.0	−63.3 ± 5.1	−63.8 ± 7.7	−55.6 ± 4.8
Dihedral ψ	−46.5 ± 8.8	−48.8 ± 7.6	−45.8 ± 8.5	−39.2 ± 5.2	−39.4 ± 8.0	−49.3 ± 5.2	−44.4 ± 6.7

Distances are given in Å. Dihedral angles are presented in degrees. The plus/minus values indicated represent one standard deviation from the mean.

Prediction of coiled-coil residues in subunit *b*

The results of sequence-based prediction of the cytosolic region of the *E. coli* subunit *b* protein performed using the *paircoil2* program (18) are summarized in Fig. 2. The figure shows the amino acid sequence of subunit *b* as well as the predicted coiled-coil heptad assignment (letters *a–g*) of those residues that had *paircoil2* P-scores that were calculated to be <0.045 (marked with an *asterisk*). The P-scores calculated by *paircoil2* estimate the probability of noncoiled-coil residues being assigned to a coiled-coil heptad position (18). The P-value cutoff of 0.045 used to create Fig. 2 suggests that each of the assigned heptad positions in the figure has at least a 95% probability of being correctly identified as a coiled-coil residue (18). The left-handed coiled-coil heptad repeat region of the *E. coli* subunit *b* identified in these experiments can be seen to persist from amino acid residue 31 through at least residue 116 (Fig. 2).

Discontinuities in the heptad repeats of left-handed coiled-coil proteins with known structures have been recognized for some time and have been discussed in detail in Brown et al. (42) (see Discussion). The predicted left-handed coiled-coil region of subunit *b* between residues 30 and 122 shown in Fig. 2 contains two stutter deletions between residues 73 and 74 and between residues 94 and 95 and a two-heptad position deletion between 116 and 117. One might expect the presence of stutters between residues 73/74 and 93/94 in subunit *b* to produce an underwinding of the supercoil in these regions, whereas the C-terminal discontinuity at residues 116/117 may terminate the coiled-coil interactions.

Simulated annealing experiments to generate subunit *b* coiled-coil structures using the ideal restraint database set and the predicted heptad repeat

The Cα to Cα distance restraints and average ϕ and ψ dihedral angle values generated with the ideal coiled-coil data set (Table 1) were used in SA runs using XPLOR-NIH to generate dimeric left-handed coiled-coil structures for the subunit *b* homodimer between residues 31 and 116 (the regions with strongly predicted heptad repeats, Fig. 2). SA was performed as for the best cortexillin I trials shown above. To accommodate the two heptad repeat stutters predicted to be present at residues 73/74 and 93/94 (Fig. 2), the Cα to Cα distance restraints for residues 71–76 and 91–96 were not specified. Experiments performed without these restraint omissions resulted in much poorer quality models as assessed by the analysis protocols described in Methods (data not shown). The restraint omissions in the regions of the subunit *b* stutters had the effect of relieving Cα to Cα distance restraint-induced stresses in the protein structure in these regions. The initial models produced by these protocols were refined as described for the cortexillin I models, and a subset of 30–40 structures with minimal violations was identified.

Fig. 3 shows the backbone helices and surface representations of the lowest energy model produced from these experiments. The left and right panels of the figure show the same representations rotated about the *y* axis by ~180°. Residues 73 and 93 (beginning of the two predicted stutters in subunit *b*) show the side-chain atoms in silver. The surface representations show the charge distribution on the surface of the dimer, with more negative charges corresponding to more intense red colors and more positive charges corresponding to more intense blue colors. The figure shows that the left-handed coiled-coil structure produced by these experiments appears to be very closely packed with a loosening of the heptad *a* and heptad *d* packing in the stutter region (residues 71–96). This latter observation is supported by analysis of the Cα to Cα distances in this model.

When Cα to Cα distances for the most closely packed heptad positions *a* and *d* in a left-handed coiled-coil are calculated from this model, the average heptad *a* Cα to Cα in the nonstutter region (residues 31–70 and 97–116) were calculated to be 7.1 ± 0.5 Å, whereas the heptad *a* Cα to Cα in the stutter region (residues 71–97) was calculated to be 8.2 ± 1.3 Å. Similarly the heptad *d* Cα to Cα in the nonstutter region was calculated to be 7.8 ± 0.6 Å, whereas the heptad

TABLE 4 Differences between the cortexillin I crystal structure and average restraint-modeled cortexillin I

Measurement	Heptad a	Heptad b	Heptad c	Heptad d	Heptad e	Heptad f	Heptad g
Distance Cα-Cα	1.4	0.1	−0.2	1.2	0.8	−0.2	0.2
Dihedral ϕ	0	4.8	7.1	−4.8	−3.0	1.4	8.6
Dihedral ψ	9.3	7.8	3.1	−1.1	0.3	6.9	2.0

Distances are given in Å. Dihedral angles are presented in degrees. The plus/minus values indicated represent one standard deviation from the mean.

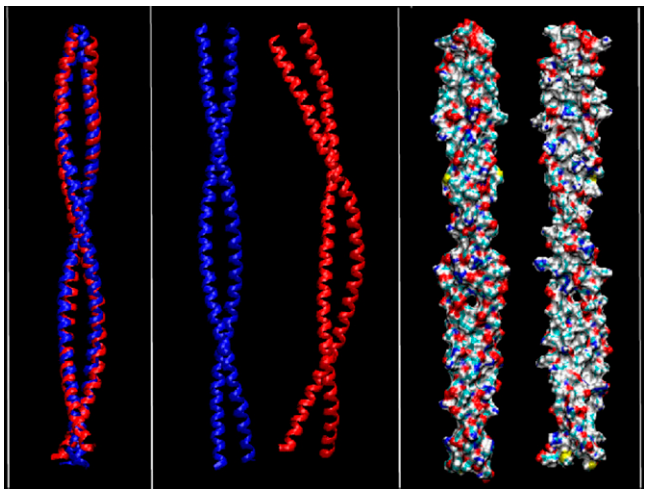

FIGURE 1 Helical structures of the modeled and crystallographically determined cortexillin I coiled-coils. Left panel: the superposed helical structures of cortexillin I modeled ab initio from amino acid sequences and average coiled-coil restraints from the ideal data set (*red*) and the structure of cortexillin I determined by x-ray crystallography by Burkhard et al. (34) in blue. The center panel shows a nonsuperposed view taken at ~90° from the first view. The right panel shows the molecular surfaces of the two structures colored by the intensity of charges on each atom (*red*: negative and *blue*: positive). Charges were calculated by the python script of Dolinsky et al. (32), and the representation was created by the MSMS program of Sanner et al. (33). Hydrogen atoms were added to the crystal structure before charge and surface calculations were made by the *psfgen* package in VMD (22). Residue 243 and residue 342 of the cortexillin I protein chains are oriented at the bottom and top in each of the figures, respectively.

a Cα to Cα in the stutter region was calculated to be 8.6 $\pm$ 1.0 Å. Although these values are within one standard deviation of each other, the loosening of the packing of *a* and *d* residues in the stutter as is suggested by our data are consistent with the predictions discussed in Brown et al. (42). The characteristics of the best model produced by these experiments are consistent with what is known about left-handed coiled-coils and suggest that the *E. coli* subunit *b*-dimerization domain can form a stable left-handed coiled-coil structure.

Experiments to determine whether or not the monomeric crystal structure determined for the *E. coli* subunit *b*-dimerization domain can be accommodated by a left-handed coiled-coil

It was of interest to determine whether the structure for a monomeric portion of the *E. coli* subunit *b* between residues 62 and 122 solved by x-ray crystallography (10) could pack as a left-handed coiled-coil structure such as those produced by the SA described above, especially since the ''slight right-handed twist'' reported in Del Rizzo et al. (10) was taken as evidence that subunit *b* adopts a dimeric right-handed coiled-coil structure (10,12). To reproduce the crystallographically determined structure of the monomer in a dimeric molecule created by SA procedures, Tcl programming scripts were developed to analyze the structure reported in Del Rizzo et al. (10). These scripts allowed the collection of interatomic distance data from the monomeric subunit *b* that was then used to create distance restraint tables for SA experiments. About 1650 distance restraints were collected for monomeric subunit *b* by identifying the backbone N, Cα, C, or O atoms that were within 6 Å of any given Cα atom and tabulating the identity of each atom and the distances between them.

These data determined on the monomer were then converted to restraint tables (with a plus/minus distance range of 10% of the determined value) for each subunit of the dimer for use in SA experiments, as described in Methods. In addition to these intrachain restraints, we utilized the interchain dimeric distance restraints (i.e., Cα-Cα distances), the ϕ and ψ dihedral restraints, and intrachain long-range Cα to Cα10 and Cα to Cα20 restraints that were previously used to produce the low-energy, left-handed coiled-coil model shown in Fig. 3. Using identical protocols, 46 structures were initially built and refined, and the lowest energy model was further analyzed.

Fig. 4 shows a superposition of the x-ray crystallographically determined structure for residues 62–122 of the *E. coli* subunit *b* monomer from Del Rizzo et al. (10) (shown in *yellow*) with the lowest energy dimeric model found in these

```
residue   1-----------------------------31-------------------------------------------------------------90
stutter                                                                  73-74
          |                             |                               ||                            |
residue   MNLNATILGQAIAFVLFVLFCMKYVWPPLM AAIEKRQKEIADGLASAERAHKDLDLAKASATDQLKKAKAEAQVIIEQANKRRSQILDEA
heptad                                  bcdefgabcdefgabcdefgabcdefgabcdefgabcdefgabfgabcdefgabcdefga
P-score                                 ************************************************************

residue   91------------------------------ 123-----------------------------156
stutter     93-94                  116-117
          | ||                     ||      |                              |
residue   KAEAEQERTKIVAQAQAEIEAERKRAREELRK QVAILAVAGAEKIIERSVDEAANSDIVDKLVAEL
heptad    bcdabcdefgabcdefgabcdefgabefgabc
P-score   *******************************
```

FIGURE 2 Predicted heptad repeats in the *E. coli* subunit *b* amino acid sequence. Heptads were predicted with the *paircoil2* program (18). Residue numbers for subunit *b* are shown in the top line. The two stutter regions (42) between residues 73 and 74 and 93 and 94 and a two-heptad position deletion between 116 and 117 are shown with hash marks pointing them out in the sequence. The third line shows the amino acid sequence of the protein, and the fourth line indicates which heptad position the amino acid is predicted to exist in. The asterisks in the fifth line point out those positions with a *paircoil2* calculated P-score value $<$0.045 ($>$95% probability of being a coiled-coil position).

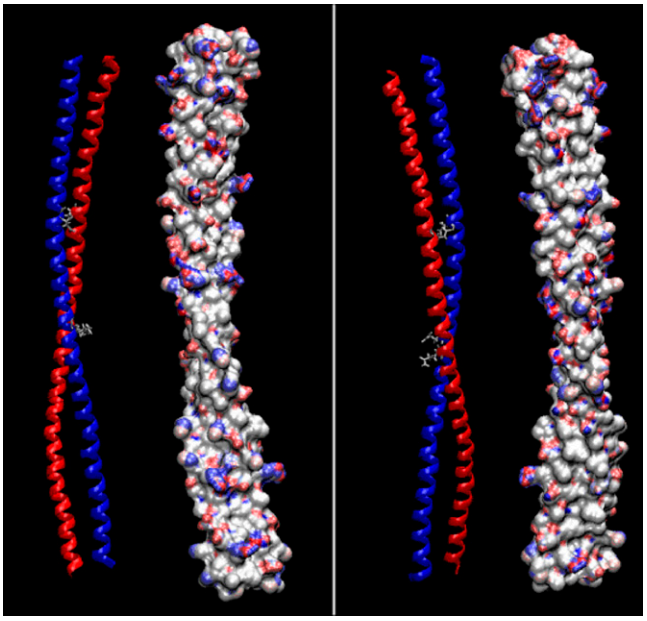

FIGURE 3 Left-handed coiled-coil model of residues 31–122 of the *E. coli* subunit *b*-dimer. The left panel shows the helical structure of the lowest energy model obtained (colored by chain; side chains marking the stutters present in the structures are shown for residues 73 and 93) and a surface representation colored by the intensity of charges on each atom (*red*: negative and *blue*: positive). Charges were calculated by the python script of Dolinsky et al. (32), and the representation was created by the MSMS program (33). The right-hand panel shows the same representations after rotation of the molecule by ~180°. Residue 31 is at the bottom of each of the representations. Note the more parallel nature of the coiled-coil in the region between the stutters.

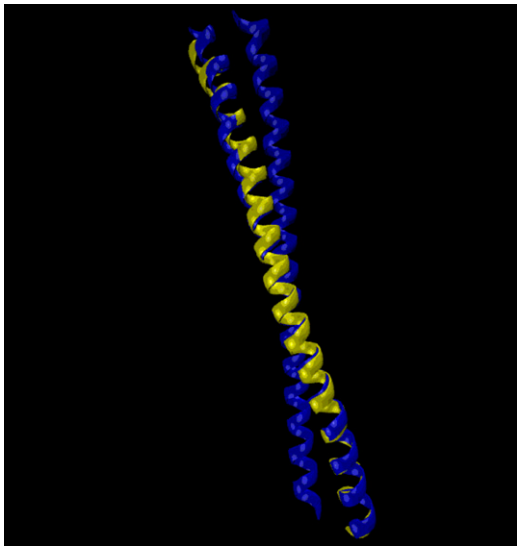

FIGURE 4 Overlay of the crystal structure for monomeric subunit *b* and a low-energy model. The x-ray crystallographically determined structure for residues 62–122 of the *E. coli* subunit *b* monomer (10) is shown in yellow, and a low-energy, left-handed coiled-coil dimeric model of subunit *b* is shown in blue. Backbone atoms for one of the chains of the dimer and the monomeric crystal structure were superposed.

experiments (shown in *blue*). The figure shows the superposed backbone atoms between residues 62 and 122 of chain *B* of the modeled subunit *b*-dimer with the crystal structure of the monomer determined in Del Rizzo et al. (10). The RMSD between backbone atoms for residues 62–122 of this model relative to the backbone atoms in 1L2P was calculated to be <1.5 Å. The results demonstrate that the structure reported in Del Rizzo et al. (10) for the monomeric *E. coli* subunit *b* can be accommodated by dimeric, left-handed coiled-coil structures.

Analysis and manipulation of the tetrameric right-handed coiled-coil tetrabrachion protein in an attempt at modeling right-handed subunit *b* coiled-coil dimers

Because it has been postulated that the *E. coli* subunit *b* protein exists in a dimeric right-handed coiled-coil structure and because there is no reported example of a dimeric coiled-coil protein in the PDB, we attempted to create ''best-guessed'' structures of such molecules to further investigate the possibility that subunit *b*-dimer exists in a right-handed coiled-coil quaternary structure. To this end the tetrabrachion right-handed coiled-coil tetramer (43) was manipulated to create hypothetical right-handed dimeric coiled-coils. To simulate a dimeric right-handed coiled-coil structure from the tetrameric structure of tetrabrachion, the two facing helices (chain A and chain B) were analyzed with respect to their shared interface. Residues 19–52 of this structure show perfect undecad repeats, and the interface between these helices is made up of the eighth, first, eighth, first, and eighth residues of the repeat. The average interchain Cα to Cα distances for the undecad positions *a, b, c, d, e, f, g, h, i, j*, and *k* were determined from this right-handed coiled-coil structure using Tcl scripts as described above.

We stipulate that these measured distances are clearly not ideal for a dimeric right-handed coiled-coil structure, since they were obtained from a tetrameric protein. Our aim in these experiments was to attempt to create a purely hypothetical right-handed dimeric subunit *b* structure by SA that was restrained by values known to exist for a known right-handed coiled-coil structure. To this end, these Cα to Cα average distances for the undecad positions in tetrabrachion were applied without any stagger as restraint distances to the undecad positions of subunit *b*, as suggested in Del Rizzo et al. (12). When combined with α-helical dihedral restraints of $-60\% \pm 15\%$ and $-40\% \pm 15\%$ degrees for ϕ and ψ dihedrals, respectively, SA experiments employing target distances that varied $\pm 25\%$ from the optimal averages, it was observed after refinement that the strongly truncated subunit *b*-dimers (only residues 60–90 were included) adopted left-handed coiled-coil structures 100% of the time (40 out of 40 acceptable SA structures).

Even when similar experiments were performed where dihedral angles restrained to the right-handed coiled-coil

values measured for the tetrabrachion structure (−64.7°, −42.1°, respectively), these same subunit *b* peptides adopted left-handed coiled-coil structures 97% of the time (38 out of 39 acceptable SA structures). One structure did show a right-handed helix cross from this set of experiments. This latter structure had 331% higher total energy in the SA experiments than the lowest energy left-handed structure determined in these experiments. This value represents slightly more than 1 standard deviation above the mean energies determined for all of the structures in this data set. In additional experiments it was observed that when the acceptable range of distance restraints on Cα atoms was decreased from ±25% to ±10%, the only acceptable structures obtained were left-handed coiled-coils.

Analysis and manipulation of the tetrameric right-handed coiled-coil tetrabrachion protein in an attempt at modeling right-handed subunit *b* coiled-coil dimers that have a staggered helical interface

Del Rizzo et al. have proposed through inferences obtained from sulfhydryl cross-linking (12) that at least the region between residues 61 and 93 requires an offset between the two monomers of at least four amino acids. To simulate such a staggered start of the structure, the tetrabrachion chains *A* and *B* that were manipulated as described above were translated relative to one another in the direction of the helical axes until the undecad *a–h* interhelical Cα to Cα were approximately equidistant. This positioning was chosen to mimic the hypothetical right-handed 30-amino acid coiled-coil structure proposed in Del Rizzo et al. (10). Care was taken in these helical translations not to move the individual helical axes closer or farther apart than the original tetrabrachion interhelical distances and not to distort either helical axis. The average interhelical *a-h* distance between homologous Cα atoms in the two chains after the translation was determined to be 6.78 ± 0.29 Å, and this value was then used as Cα to Cα restraints in subsequent SA experiments.

In these attempts, the interhelical Cα to Cα atom distances from subunit *b* residue pairs a61-h68, h68-a72, a72-h79, h79-a83, and a83-h90 (as in subunit b_c and subunit b_n as designated in Del Rizzo et al. (12) were restrained to 6.78 Å ± 25%, and the ϕ and ψ dihedrals were restrained to the right-handed coiled-coil optimum values (−64.7% and −42.1% ± 10%) as determined for the tetrabrachion structure. When SA experiments were performed using the subunit *b*-sequence and undecad alignment as proposed in Del Rizzo et al. (12), 40 acceptable dimeric structures were obtained. Of these structures, 20 were right-handed (50%), 18 were left-handed (45%), and 2 were parallel with no perceptible helical crossing as judged by visual analysis. These results demonstrated that geometrically acceptable protein coils could be obtained from SA experiments that had either left- or right-handed helical crossings.

It is worth noting that the peptides used by Del Rizzo and co-workers in their disulfide oxidation experiments on truncated subunit *b* proteins contained an Arg-83 to Ala mutation (12), previously reported by these authors to stabilize the dimeric structure of the soluble *b* peptides (10). In SA experiments performed here that were identical to those reported above except that the *b* proteins carried the Arg-83Ala mutation, 46 acceptable subunit *b*-dimer structures were obtained. Of these structures, 27 displayed right-handed helical crossing (59%) and 19 were observed to cross in a left-handed manner (41%). The lowest energy structure from these experiments was a right-handed coiled-coil. There seems to be no greatly observable effect of the Arg-83Ala mutation in these experiments, i.e., there appeared to be no great difference in the ease of packing the Arg-83Ala mutant proteins into right-handed coiled-coils versus left-handed coiled-coils in these SA studies.

Do staggered right-handed coiled-coil structures explain interchain disulfide formation better than staggered left-handed coiled-coil structures?

Each of the best 40 staggered structures produced as described above was analyzed for the interchain distance between the Cα positions at positions 61/68, 68/72, 72/79, 79/83, and 83/90, which were reported by Del Rizzo and co-workers to produce the highest yield of interchain disulfide bonds (12). Left- and right-handed structures were identified by visual analysis, and Cα to Cα distances and Cβ to Cβ distances for these atom pairs were tabulated using Tcl scripts run in VMD. The right-handed coiled-coils showed average interchain Cα distances and standard deviations for residue pairs 61/68, 68/72, 72/79, 79/83, and 83/90 equal to 8.2 ± 0.5, 8.0 ± 0.6, 7.8 ± 0.8, 7.7 ± 0.7, and 8.4 ± 0.3 Å, respectively. The left-handed respective values were 8.4 ± 0.3, 8.2 ± 0.4, 7.9 ± 0.8, 7.8 ± 0.7, and 8.5 ± 0.1. These calculations suggested that there were no significant differences between the average distances between Cα atoms (or Cβ atoms, data not shown) when staggered left-handed helices were compared with staggered right-handed helices. This result has important implications for arguments that use the reported disulfide cross-linking results as evidence for right-handed coiled-coil *b*-dimer structures.

These data, although suggesting that either left- or right-handed coiled-coil structures might accommodate the disulfide-formation data reported in Del Rizzo et al. (12), are not definitive since the interchain distances observed in the SA-produced structures were larger than that believed to be typical for cystine disulfide bonds. Petersen and colleagues (44) have presented a comprehensive analysis of cystine conformations using a database of 351 disulfide bridges determined for 131 different proteins and have reported the most common Cα to Cα distance for these cystines to be equal to 5.8 Å. In an attempt to create a more rigorous test of whether staggered left- and/or right-handed coiled-coil

structures based on the subunit *b*-sequence best accommodate the disulfide-formation experiments, a further set of SA experiments analogous to those in the previous section were performed.

In these experiments, the interchain distances between residue pairs 61/68, 68/72, 72/79, 79/83, and 83/90 were restrained to a rigorous 5.8 ± 0.1 Å, and dihedral angles were restrained to values favorable to the formation of right-handed coiled-coils (as above). After refinement and analysis of model quality as described in Methods, 46 structures were found to be acceptable. Of these structures, 22 (48%) were found by visual analysis to have right-handed helical crosses and 9 (20%) were observed to have left-handed helical crosses with the remainder having no detectable crossing pattern. Again, the results demonstrated that either left-handed or right-handed helix crossing in the resultant structures could accommodate the disulfide cross-linking results.

Mixed left-handed coiled-coil and staggered right-handed coiled-coil models of the subunit *b*-dimer

Finally, we attempted to create complete α-helical subunit *b* structures that included left-handed coiled-coil restraints for residues 30–58, right-handed staggered coiled-coil restraints for residues 60–90, and again left-handed restraints for residues 93–117. The right-handed coiled-coil restraints with the inclusion of the proposed stagger were as described above, and left-handed restraints were as described above for Fig. 3. Three geometrically acceptable structures were obtained. All three structures were completely left-handed throughout all restrained regions. All three structures accommodated the staggered region between residues 60 and 90 but with a left-handed coiled-coil structure.

DISCUSSION

This work attempts to address important questions about the structure of the *E. coli* ATP synthase external stalk. Structural modeling of the subunit *b*-dimer in a dimeric left-handed coiled-coil form was performed with the SA approach first used by Nilges and Brünger (20) and based on the theoretical predictions of heptad repeats first proposed by Crick (11).

Specific questions have arisen as a consequence mainly of the research reported by Dunn and co-workers that has principally been reported in Del Rizzo et al. (10,12). The structure observed in the diffraction studies (10) was short (residues 62–122) and monomeric. They reported that ''most of the hydrophobic residues in the $b_{62\text{-}122}$ monomer are arranged in a strip along the surface of the α-helical axis'' and that because this strip ''moves around the helix in a right-handed sense'', they aligned the two strips of a theoretical dimer visually into a hypothetical coiled-coil with a right-handed superhelical twist (10). In more recent work, these researchers identified an 11-residue repeat in putative packing residues in subunit *b* and reported on a series of disulfide bond-formation experiments using very short, mutant subunit *b* proteins to extend support for their hypothesis that subunit *b* exists as a right-handed dimeric coiled-coil complex (12).

Right-handed coiled-coils have been observed in trimeric and four-helical bundle systems, but stable dimeric right-handed coiled-coils have not yet been observed. The stabilities of artificially designed dimeric, trimeric, and four-helical bundled right-handed coiled-coils have been examined by Kim and co-workers (see, for example, Harbury et al. (19)), but even in these systems no stable right-handed coiled-coil dimers have been observed in either NMR or crystallographic studies. Close examination of the transmembraneous right-handed dimeric structure of glycophorin A in detergent micelles (45) reveals a helical crossing angle of close to 40°, which is inconsistent with a true coiled-coil structure and is closer to the 50° helix packing angles observed in noncoiled-coil, α-helical proteins like the globins.

Reasonable heptad repeats are identified in subunit *b* packing interfaces

Crystallographic analyses of classical left-handed coiled-coil proteins have revealed heptad repeats (*a, b, c, d, e, f, g*) in the sequence of these proteins with apolar residues chiefly present in the *a* and *d* positions (42). Refinements have recently been made in predictive algorithms that have been used to identify heptad repeats, the most recent of which was reported by McDonnell et al. (18), who have extensively trained and tested their algorithm with known coiled-coil structures from the PDB. Analysis of the *E. coli* subunit *b*-sequence with *paircoil2* allowed us to identify typical left-handed coiled-coil heptad repeats between residues 31 and 122 (Fig. 2). We observed a continuous stretch of identified heptad positions between these residues that was interrupted by two discontinuities between residues 73 and 74 and between residues 93 and 94, with a third discontinuity occurring between residues 116 and 117. The first two discontinuities were of the three-residue deletion type termed ''stutters'' by Brown et al. (42). These are the most commonly observed discontinuities seen in coiled-coils and produce interhelical packing in the vicinity of the stutter that is not as tight as that observed in uninterrupted heptad repeat regions (42). Stutters may serve to increase the flexibility of the coiled-coil structures in which they are found or to help terminate the coiled-coil interface (42).

The presence of a stutter also results in an underwinding of the coiled-coil (increase in pitch length), and an imperfect form of side-chain packing between helices in these regions occurs (42). It seems reasonable to conclude, in light of the work of Brown et al. (42), that the stutters predicted between residues 73/74 and 93/94 of the *E. coli* subunit *b* likely serve to produce an underwinding in this region of the coiled-coil and that the discontinuity found at residues 116 and 117 at the C-terminal end of the predicted left-handed coiled-coil helps

terminate the coiled-coil interactions. An interesting, independent observation that seems to nicely support the positioning of the stutters in subunit *b* stems from earlier data from our lab (46). These electron spin resonance studies showed close interaction of the *b*-dimer with soluble F_1 starting just above residue 80 (which is just C-terminal to the first stutter). The close interaction shown with F_1 in Motz et al. (46) then ends at about *b* amino acid 100, just above the second stutter. The inclusion of the stutters in subunit *b* may have served to create specific F_1-interaction surfaces in the more underwound part of the coiled-coil stator.

We conclude from our analyses of putative heptad repeats in the subunit *b*-sequence and from what is known about interruptions in these repeats (42) that a viable heptad repeat alternative exists to the undecad repeat identified by Del Rizzo and co-workers (12).

Subunit *b* can adopt a conventional left-handed coiled-coil structure

In our structural modeling experiments, the coiled-coil heptads' positions predicted by *paircoil2* and earlier algorithms (16) were used with distance and dihedral angle data sets that were extracted from known left-handed coiled-coils to compile average distance and dihedral angle values for left-handed coiled-coil heptad positions (Table 1). The utility of these average values was demonstrated by the calculation of SA models of the left-handed dimeric coiled-coil, cortexillin I (Fig. 1). The theoretical model of cortexillin I correlated very well with the x-ray crystallographic structure of this protein (34). The measured Cα to Cα distances between like heptad positions in the SA-modeled versus crystallized cortexillin I were observed to be within 1.4 Å and the deviation of dihedral angle values $<$10% (Fig. 1 and Tables 2–4).

The *paircoil2*-predicted heptad assignments between residues 31 and 116 of the *E. coli* subunit *b* (Fig. 2) were used in SA calculations with the best combination of ideal coiled-coil restraint data identified in the test results using the cortexillin I structure. To accommodate possible loosening of the packing between the helices caused by the stutters in the *E. coli* subunit *b*-sequence at residues 73/74 and 93/94, Cα to Cα distance restraints were omitted between residues 71–76 and 91–96. Acceptable models were obtained (Fig. 3) that appear to have very close packing between monomers with the expected loosening of the packing in the stutter regions as assessed by analysis of the Cα to Cα distances in the respective regions. The quality of these theoretical models of dimeric, left-handed coiled-coil subunit *b* structures strongly suggests that this form of the dimer would be a stable structure.

The crystal structure reported for subunit *b* monomer fits a left-handed coiled-coil dimer

We then determined whether or not the monomeric structure of subunit *b* determined by x-ray crystallography (10) could be accommodated in a left-handed coiled-coil dimer. We collected intramonomer distance restraints from the crystal structure and used these data in SA experiments together with the distance restraints and dihedral angle restraints for left-handed coiled-coils as described above. All models produced from these calculations were left-handed dimeric coiled-coils. The best of these models (lowest energy with no geometry violations) was superposed on the crystal structure of *b*. The RMSD between backbone atoms for the model and the crystal structure was $<$1.5 Å. These experiments demonstrated that the reported crystal structure of subunit *b* monomer can be accommodated in a classical, dimeric, left-handed coiled-coil (Fig. 4).

Theoretical modeling of hypothetical, nonstaggered, right-handed dimeric coiled-coils

Modeling right-handed coiled-coil dimers utilized an SA approach similar to that employed in making the left-handed models. Since no known dimeric structure exists that could be used as an ideal structure for measurement of restraint data, the tetrameric right-handed coiled-coil tetrabrachion structure (43) was used for analysis. Two facing helices from chains *A* and *B* that show perfect undecad repeat were analyzed, and averaged Cα to Cα distances and ϕ/ψ dihedral angles were calculated and applied in restraint tables to subunit *b* by using the undecad positions reported in Del Rizzo et al. (12). Although only a very short amino acid stretch of 31 amino acids (amino acids 60–90) was restricted by these restraints, nearly all of the resultant structures showed left-handed supercoiling. The one structure observed to possess a right-handed helical crossing was much higher in energy than the left-handed coils. This energy difference was principally the result of a much higher effective nuclear Overhauser effect and dihedral energy terms as calculated by XPLOR-NIH (21- and 175-fold higher, respectively) for the right-handed versus left-handed coiled-coil structures. The lack of production of many right-handed coiled-coils may have been due to the lack of better information on which to base the restraint tables. An alternative explanation might be that right-handed, dimeric coiled-coil structures based on unstaggered subunit *b* are not as stable as left-handed, unstaggered coiled-coils.

Hypothetical right-handed dimeric coiled-coils with staggered starts

To test the hypothesis from Dunn and co-workers that the subunit *b*-dimer exists in a staggered, right-handed coiled-coil, we carefully translated the *A* and *B* chains of the tetrameric tetrabrachion protein relative to one another to make the interhelical undecad *a* and *h* Cα to Cα distances approximately equidistant, as suggested by the hypothetical figure shown in Fig. 1 of Del Rizzo et al. (12). After determining the average distance between *a* and *h* Cα atoms, this value

was used as described for Fig. 3 in SA experiments using the truncated *b*-peptide sequences. These calculations were more successful in generating right-handed coiled-coils, with about half of the geometrically acceptable models possessing helical crossings in a right-handed sense and ~45% crossing in a left-handed fashion.

The production of both left- and right-handed coiled-coils from these experiments proved fortuitous in that it allowed the comparison of the two staggered structures with respect to reported disulfide cross-linking results performed on truncated subunit *b* mutants (see next section). That there was no preferential stabilization of right-handed coils by the Arg-83Ala mutation previously reported to stabilize dimeric interactions (10) may reflect the fact that the *paircoil2* predictions for subunit *b* identified Arg-83 as an interfacial, heptad *a* residue of a left-handed coil (Fig. 2). Arg-83Ala might stabilize the left-handed coiled-coil interface by replacing the bulky Arg with the much smaller Ala side chain. That Arg may be used in the normal, unmutated proteins likely reflects the apolar nature of the Cβ, Cγ, and Cδ methylene groups of the wild-type arginine residue.

Is a staggered start in the coiled-coil necessary for structural stability of the subunit *b*-dimer?

One of the arguments used to support the contention that the subunit *b*-dimerization domain adopts a dimeric right-handed coiled-coil relies on inferences obtained from sulfhydryl cross-linking studies performed on short, truncated *b*-subunits composed of residues 53–122 or 62–122 (12). It was suggested that an offset of interfacial amino acids is required to explain the interesting lack of homodimeric disulfides formed between residues 79/79, 83/83, and 90/90 and the ''essentially complete disulfide formation'' seen for residues 61/68, 68/72, 72/79, 79/83, and 83/90 (12). There was ''modest'' homodisulfide formation reported (12) between residues 61/61, 68/68, and 72/72. To explain these results, a structural scheme that requires the subunit *b*-dimer to form an offset, right-handed coiled-coil that exhibits an undecad repeat to form the theoretical hydrophobic interaction surface between the hypothetical monomers was proposed (12). The webtool REPPER FTwin (47) was reported to have identified such an undecad repeat in the subunit *b*-sequence between residues 53 and 122 (12). The authors argue that only the undecad repeat of the right-handed coiled-coil can be used to position the hydrophobic interface residues (undecad *a* and *h* residues, in Del Rizzo's nomenclature) close enough at the 68(*h*)/72(*a*), 72(*a*)/79(*h*), 79(*h*)/83(*a*), and 83(*a*)/90(*h*) to explain the ''essentially complete disulfide formation'' at these positions.

Our experiments showed that, indeed, unstaggered 68/68–90/90 disulfide formation would not be favorable since the best model obtained in our molecular modeling investigations positions these residues in geometrically unfavorable positions for disulfide formation. Due to the stutter that is predicted by *paircoil2* at amino acids 73/74, these cross-linked, staggered amino acids are indeed on the inner helix surface. An alternative to a stable staggered right-handed coiled-coil may then be that disulfide cross-link formation occurred by simple sliding of the short peptides relative to each other during the long 24-h period (see Del Rizzo et al. (12)) allowed for reaction. In an attempt to create less truncated models, inclusion of left-handed coiled-coil restraints was indicated in Fig. 2 but with right-handed staggered restraints for residues 60–90, as postulated for subunit *b* in Del Rizzo et al. (12), resulting in the identification of only left-handed staggered models. These results suggested that there is no readily accessible physical solution to simultaneously including both left- and right-handed helical crossing directions in one structure.

CONCLUSIONS

We have identified an extensive heptad repeat between residues 31 and 116 of the *E. coli* subunit *b*-sequence that is consistent with the interface packing of protein side chains in a classical dimeric, left-handed, coiled-coil structure, a geometry first suggested by Crick (11). This heptad repeat contains two stutters at residues 73/74 and 93/94; and in accord with the work of Brown et al. (42), we hypothesized that these stutters loosen the coiled-coil packing interactions between the helices in these regions and may allow favorable interaction with the F_1-ATPase section of the ATP synthase. This left-handed coiled-coil heptad repeat appears to be a reasonable alternative to the right-handed coiled-coil undecad repeat proposed for subunit *b* in Del Rizzo et al. (12). We have shown using SA computations that the *E. coli* subunit *b* protein based on the identified heptad repeat can adopt an unstaggered, dimeric, left-handed coiled-coil quaternary structure that is geometrically and energetically stable.

Superposition of unstaggered left-handed coiled-coil subunit *b*-dimer models created in our SA experiments based on the x-ray structure of the monomeric *b* (10) strongly suggests that left-handed coiled-coil dimerization of *E. coli b* may well take place. This same x-ray structure led the authors to the assumption of a right-handed supercoil of the dimer (10). We have, in addition, shown that truncated versions of the *E. coli* subunit *b*-dimer could in some cases adopt hypothetical right-handed coiled-coil structures with or without a staggered start and that acceptable left-handed versions of the short coiled-coils could also be created. The disulfide cross-linking experiments as reported in Del Rizzo et al. (12) can be accommodated by structurally acceptable staggered coiled-coils that possess either left-handed or right-handed supercoiling. We have shown that the cross-linking data discussed in Del Rizzo et al. (12) provide no evidence on the direction of supercoiling in the subunit *b*-dimer.

This work has shown that the subunit *b*-dimer can reasonably adopt a classic, left-handed coiled-coil structure and

that this structure can accommodate the available biochemical and biophysical evidence that has accumulated for subunit *b*. Whether or not there is potential for some parts of the subunit *b*-dimer to form right-handed coiled-coil structures remains an intriguing question that may have mechanistic implications that have, as of yet, no direct experimental support. We speculate that the subunit *b*-dimer exists in a stable left-handed coiled-coil structure in its low-energy state but that during rotation of the ATP synthase *c*-subunits relative to the *b*-dimer the left-handed supercoiling of *b* may become lessened to a more underwound parallel state, which may perhaps even transiently adopt a right-handed coiled-coil state. Whether this higher energy state at intermediate stages during rotation would be sufficient to function as an elastic counterbalance to help gear the smaller c-rotation steps to the larger rotational substeps of subunit γ remains to be seen.

The authors acknowledge the support of Joseph Gargiula, Abby Kinney, Allen Hughes, Shirlene Pearson, David Alley, James Jaeger, and Randall Powell of the Information Technology Services at Southern Methodist University for supplying the computers used in this work and to Justin Ross and Tristan Ziska for their invaluable competence in setting up and maintaining the computing cluster. The authors also thank Larry Ruben (Department of Biological Sciences at SMU) for support and space for the cluster, Steven Vik for allowing us a prepublication look at his review, Mark Girvin (Albert Einstein College of Medicine) for initial advice with simulated annealing protocols, and Ben Wise and Eric Wise for their assistance in setting up the cluster.

This work was funded by a grant from the National Science Foundation (MCB 0415713) to P.D.V.

REFERENCES

1. Walker, J. E. 1998. ATP synthesis by rotary catalysis. *Angew. Chem. Int. Ed.* 37:2308–2319.
2. Boyer, P. D. 1998. ATP synthase—past and future. *Biochim. Biophys. Acta.* 1365:3–9.
3. Senior, A. E., S. Nadanaciva, and J. Weber. 2002. The molecular mechanism of ATP synthesis by F1F0-ATP synthase. *Biochim. Biophys. Acta.* 1553:188–211.
4. Vik, S. B. 2007. ATP synthesis by oxidative phosphorylation. *In*: EcoSal—*Escherichia coli* and *Salmonella*: Cellular and Molecular Biology. A. Böck, R. Curtiss III, J. B. Kaper, P. D. Karp, F. C. Neidhardt, T. Nyström, J. M. Slauch, and C. L. Squires, editors. [Online.] http://www.ecosal.org.
5. Duncan, T. 2004. The ATP synthase: parts and properties of a rotary motor. *In*: The Enzymes: Energy Coupling and Molecular Motors. D. Hackney and F. Tamanoi, editors. 203–275.
6. Capaldi, R. A., and R. Aggeler. 2002. Mechanism of the F1F0-type ATP synthase, a biological rotary motor. *Trends Biochem. Sci.* 27:154–160.
7. Weber, J. 2006. ATP synthase: subunit-subunit interactions in the stator stalk. *Biochim. Biophys. Acta.* 1757:1162–1170.
8. Walker, J. E., and V. K. Dickson. 2006. The peripheral stalk of the mitochondrial ATP synthase. *Biochim. Biophys. Acta.* 1757:286–296.
9. Dmitriev, O., P. C. Jones, W. Jiang, and R. H. Fillingame. 1999. Structure of the membrane domain of subunit *b* of the Escherichia coli F0F1 ATP synthase. *J. Biol. Chem.* 274:15598–15604.
10. Del Rizzo, P. A., Y. Bi, S. D. Dunn, and B. H. Shilton. 2002. The ''second stalk'' of Escherichia coli ATP synthase: structure of the isolated dimerization domain. *Biochemistry.* 41:6875–6884.
11. Crick, F. H. C. 1953. The packing of alpha-helices: simple coiled-coils. *Acta Crystallogr.* 6:689–697.
12. Del Rizzo, P. A., Y. Bi, and S. D. Dunn. 2006. ATP synthase *b* subunit dimerization domain: a right-handed coiled coil with offset helices. *J. Mol. Biol.* 364:735–746.
13. Steigmiller, S., M. Börsch, P. Gräber, and M. Huber. 2005. Distances between the b-subunits in the tether domain of F0F1-ATP synthase from E. coli. *Biochim. Biophys. Acta.* 1708:143–153.
14. Lupas, A., M. Van Dyke, and J. Stock. 1991. Predicting coiled coils from protein sequences. *Science.* 252:1162–1164.
15. Berger, B., D. B. Wilson, E. Wolf, T. Tonchev, M. Milla, and P. S. Kim. 1995. Predicting coiled coils by use of pairwise residue correlations. *Proc. Natl. Acad. Sci. USA.* 92:8259–8263.
16. Wolf, E., P. S. Kim, and B. Berger. 1997. MultiCoil: a program for predicting two- and three-stranded coiled coils. *Protein Sci.* 6:1179–1189.
17. Delorenzi, M., and T. Speed. 2002. An HMM model for coiled-coil domains and a comparison with PSSM-based predictions. *Bioinformatics.* 18:617–625.
18. McDonnell, A. V., T. Jiang, A. E. Keating, and B. Berger. 2006. Paircoil2: improved prediction of coiled coils from sequence. *Bioinformatics.* 22:356–358.
19. Harbury, P. B., B. Tidor, and P. S. Kim. 1995. Repacking protein cores with backbone freedom: structure prediction for coiled coils. *Proc. Natl. Acad. Sci. USA.* 92:8408–8412.
20. Nilges, M., and A. T. Brünger. 1993. Successful prediction of the coiled coil geometry of the GCN4 leucine zipper domain by simulated annealing: comparison to the x-ray structure. *Proteins.* 15:133–146.
21. Charest, G., and P. Lavigne. 2006. Simple and versatile restraints for the accurate modeling of alpha-helical coiled-coil structures of multiple strandedness, orientation and composition. *Biopolymers.* 81:202–214.
22 Humphrey, W., A. Dalke, and K. Schulten. 1996. VMD: visual molecular dynamics. *J. Mol. Graph.* 14:33–38, 27–28.
23. Ousterhout, J. C. 1994. Tcl and the Tk Toolkit. Addison-Wesley Professional, Upper Saddle River, NJ.
24. Sanner, M. F. 1999. Python: a programming language for software integration and development. *J. Mol. Graph. Model.* 17:57–61.
25. Schwieters, C. D., J. J. Kuszewski, N. Tjandra, and G. M. Clore. 2003. The Xplor-NIH NMR molecular structure determination package. *J. Magn. Reson.* 160:65–73.
26. Schwieters, C. D., J. J. Kuszewski, and G. M. Clore. 2006. Using Xplor-NIH for NMR molecular structure determination. *Prog. Nucl. Magn. Reson. Spectrosc.* 48:66–74.
27. Nilges, M., J. Kuszewski, and A. T. Brünger. 1991. Sampling properties of simulated annealing and distance geometery. *In* Computational Aspects of the Study of Biological Macromolecules by NMR. J. C. Hoch, F. M. Poulsen, and C. Redfield, editors. New York. 451–455.
28 Brünger, A. 1992. X-PLOR: A System for X-ray Crystallography and NMR. Yale University Press, New Haven, CT.
29. Morris, A. L., M. W. MacArthur, E. G. Hutchinson, and J. M. Thornton. 1992. Stereochemical quality of protein structure coordinates. *Proteins.* 12:345–364.
30. Laskowski, R. A., J. A. Rullmannn, M. W. MacArthur, R. Kaptein, and J. M. Thornton. 1996. AQUA and PROCHECK-NMR: programs for checking the quality of protein structures solved by NMR. *J. Biomol. NMR.* 8:477–486.
31. Phillips, J. C., R. Braun, W. Wang, J. Gumbart, E. Tajkhorshid, E. Villa, C. Chipot, R. D. Skeel, L. Kalé, and K. Schulten. 2005. Scalable molecular dynamics with NAMD. *J. Comput. Chem.* 26:1781–1802.
32. Dolinsky, T. J., J. E. Nielsen, J. A. McCammon, and N. A. Baker. 2004. PDB2PQR: an automated pipeline for the setup of Poisson-Boltzmann electrostatics calculations. *Nucleic Acids Res.* 32:W665–W667.
33. Sanner, M. F., A. J. Olson, and J. C. Spehner. 1996. Reduced surface: an efficient way to compute molecular surfaces. *Biopolymers.* 38:305–320.

34. Burkhard, P., R. A. Kammerer, M. O. Steinmetz, G. P. Bourenkov, and U. Aebi. 2000. The coiled-coil trigger site of the rod domain of cortexillin I unveils a distinct network of interhelical and intrahelical salt bridges. *Structure*. 8:223–230.

35. Day, C. L., and T. Alber. 2000. Crystal structure of the amino-terminal coiled-coil domain of the APC tumor suppressor. *J. Mol. Biol*. 301: 147–156.

36. Strelkov, S. V., H. Herrmann, N. Geisler, T. Wedig, R. Zimbelmann, U. Aebi, and P. Burkhard. 2002. Conserved segments 1A and 2B of the intermediate filament dimer: their atomic structures and role in filament assembly. *EMBO J*. 21:1255–1266.

37. Sironi, L., M. Mapelli, S. Knapp, A. De Antoni, K. Jeang, and A. Musacchio. 2002. Crystal structure of the tetrameric Mad1-Mad2 core complex: implications of a 'safety belt' binding mechanism for the spindle checkpoint. *EMBO J*. 21:2496–2506.

38. Brown, J. H., K. H. Kim, G. Jun, N. J. Greenfield, R. Dominguez, N. Volkmann, S. E. Hitchcock-DeGregori, and C. Cohen. 2001. Deciphering the design of the tropomyosin molecule. *Proc. Natl. Acad. Sci. USA*. 98:8496–8501.

39. Dumas, J. J., E. Merithew, E. Sudharshan, D. Rajamani, S. Hayes, D. Lawe, S. Corvera, and D. G. Lambright. 2001. Multivalent endosome targeting by homodimeric EEA1. *Mol. Cell*. 8:947–958.

40. Li, Y., J. H. Brown, L. Reshetnikova, A. Blazsek, L. Farkas, L. Nyitray, and C. Cohen. 2003. Visualization of an unstable coiled coil from the scallop myosin rod. *Nature*. 424:341–345.

41. Schnell, J. R., G. Zhou, M. Zweckstetter, A. C. Rigby, and J. J. Chou. 2005. Rapid and accurate structure determination of coiled-coil domains using NMR dipolar couplings: application to cGMP-dependent protein kinase Ialpha. *Protein Sci*. 14:2421–2428.

42. Brown, J. H., C. Cohen, and D. A. Parry. 1996. Heptad breaks in alpha-helical coiled coils: stutters and stammers. *Proteins*. 26:134–145.

43. Stetefeld, J., M. Jenny, T. Schulthess, R. Landwehr, J. Engel, and R. A. Kammerer. 2000. Crystal structure of a naturally occurring parallel right-handed coiled coil tetramer. *Nat. Struct. Biol*. 7:772–776.

44. Petersen, M. T., P. H. Jonson, and S. B. Petersen. 1999. Amino acid neighbours and detailed conformational analysis of cysteines in proteins. *Protein Eng*. 12:535–548.

45. MacKenzie, K. R., and D. M. Engelman. 1998. Structure-based prediction of the stability of transmembrane helix-helix interactions: the sequence dependence of glycophorin A dimerization. *Proc. Natl. Acad. Sci. USA*. 95:3583–3590.

46. Motz, C., T. Hornung, M. Kersten, D. T. McLachlin, S. D. Dunn, J. G. Wise, and P. D. Vogel. 2004. The subunit *b* dimer of the F0F1-ATP synthase: interaction with F1-ATPase as deduced by site-specific spin-labeling. *J. Biol. Chem*. 279:49074–49081.

47. Gruber, M., J. Söding, and A. N. Lupas. 2005. REPPER—repeats and their periodicities in fibrous proteins. *Nucleic Acids Res*. 33:W239–W243.